PHYSICAL REVIEW B **85**, 144416 (2012)

Quantum spin state in the rare-earth compound $YbAl_3C_3$

K. Hara, S. Matsuda, E. Matsuoka, K. Tanigaki, and A. Ochiai*
Department of Physics, Tohoku University, Sendai 980-8578, Japan

S. Nakamura and T. Nojima
Institute for Materials Research, Tohoku University, Sendai 980-8577, Japan

K. Katoh
Department of Applied Physics, National Defense Academy, Yokosuka 239-8686, Japan
(Received 28 October 2011; published 20 April 2012)

Magnetic properties of $YbAl_3C_3$ with the hexagonal $ScAl_3C_3$-type structure have been investigated by the magnetization (M) and specific-heat (C) measurements under magnetic fields (H). $YbAl_3C_3$ is reported to show a spin-gap state, which is considered to be ascribed to a magnetic dimer formed in the orthorhombic phase below the structural transition temperature ($T_s = 77$ K). Present study has revealed history-dependent magnetic properties below T_s and field-induced anomalous magnetic states at low temperatures. The former is considered to be attributed to the cross correlation between the structural deformation and the magnetic field similar to those observed in multiferroic materials, although $YbAl_3C_3$ below T_s is not in the ferromagnetic state but certainly in the dimer state. The latter is partially similar to that observed in the field-induced ordered phase (FIOP) of d-electron dimer systems. The M versus H curve at low temperatures exhibits a kink at a certain magnetic field and then it increases in proportion to the field like that of FIOP. However, neither kink nor peak suggesting the emergence of FIOP is observed in the temperature dependence of both $M(T)$ and $C(T)$. Instead, C/T shows an anomalous increase proportional to $-\ln T$ with decreasing temperature in a finite field range, suggesting an anomalous disordered state such as a non-Fermi-liquid state in a strongly correlated f-electron system. These anomalous magnetic states may be partially relevant to characteristics of f-electron dimer system.

DOI: 10.1103/PhysRevB.85.144416 PACS number(s): 75.10.Kt, 75.80.+q

I. INTRODUCTION

Quantum spin systems have attracted much attention of many researchers because of novel ground and excited states strongly influenced by quantum fluctuations. They have been intensively studied particularly in d-electron compounds, which are in a marked contrast to the case of $4f$-electron quantum spin systems. Although quantum effects are significant in a low spin system such as an $S = 1/2$ spin system, the total angular momentum J, which represents magnetic ground states of the $4f$-electron compounds, is usually much larger than $1/2$. Furthermore, most of the $4f$-electron compounds investigated by many researchers have a considerable number of conduction electrons that mediate the three-dimensional Ruderman-Kittel-Kasuya-Yosida (RKKY) interaction, which collides with another criterion of the low dimensionality for the quantum spin systems.

In real $4f$-electron materials with the structural low dimensionality, the crystalline electric field (CEF) lifts the degeneracy of the total angular momentum J, which may cause a Kramers doublet ground state for an odd-number $4f$-electron system. If the doublet ground state is well isolated from excited states, the $4f$-electron system is expected to behave as the $S = 1/2$ spin system. However, the exchange interaction sometimes overcomes the CEF splitting energy, leading to the magnetically ordered state of the classical spin system with a large degeneracy. The magnitude of the exchange interaction in the $4f$-electron compounds is conjectured by the de Gennes factor, which becomes smallest in the $4f^1$ or $4f^{13}$ configuration. Therefore, taking the above mentioned into consideration, an insulating Ce-based or Yb-based compound with low symmetric structure is considered to be an appropriate candidate for the quantum spin system in principle, although the $4f$-electron quantum spin system is quite rare.

Among the $4f$-electron compounds, Yb_4As_3 is one of the exceptional cases where a typical one-dimensional $S = 1/2$ Heisenberg antiferromagnet is realized in the charge ordered state.[1] This compound seems to satisfy two criteria for the quantum spin system, i.e., (i) the low dimensionality of the exchange interaction secured by both structural low dimensionality and low carrier concentration and (ii) a doublet ground state well isolated from excited states. Recently, $YbAl_3C_3$ joins the family of the quantum spin systems in the $4f$-electron compounds.

$YbAl_3C_3$ has the hexagonal $ScAl_3C_3$-type structure (space group $P6_3/mmc$) shown in Fig. 1(a) at room temperature where the Yb layer on the c plane is isolated by the Al and C atoms from the next Yb layer by a distance of about 8.56 Å , consequently forming a two-dimensional triangular lattice of magnetic Yb^{3+} ions,[2] i.e., a geometrically frustrated magnet. This compound shows a structural phase transition at $T_s = 77$ K to the orthorhombic phase although the crystal deformation is very tiny.[3–5] The magnetic ground state of $YbAl_3C_3$ seems to satisfy the above-mentioned two criteria for the quantum spin system, i.e., the low dimensionality of the exchange interaction secured by both structure and low carrier concentration ($1/100$ per Yb^{3+} ion) and the Kramers doublet ground state isolated from the first excited state by the CEF splitting energy of about 200 K.[6] The most interesting feature of this compound is the absence of the long-range magnetic order, which is attributed to the formation of the spin-gap

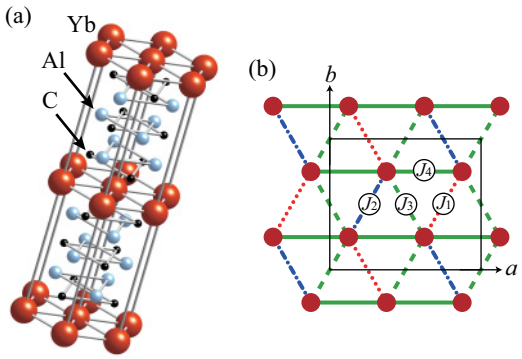

FIG. 1. (Color online) (a) Crystal structure of $YbAl_3C_3$. (b) Yb atoms on the $z = 0$ plane are shown. The rectangle drawn by the solid black line shows an orthorhombic unit cell in the low-temperature phase below T_s. J_1, J_2, J_3, and J_4 indicate four different types of the Yb-Yb bonds of the orthorhombic structure, respectively.

state with $\Delta \approx 15$ K.[3,6] Such a spin-gap state is considered to originate in the dimerization of the magnetic Yb^{3+} pair because the physical properties of $YbAl_3C_3$ are roughly explained by the isolated dimer model with the singlet-triplet splitting of 15 K.

If the spin dimer state is actually realized in $YbAl_3C_3$, the application of the magnetic field on it is expected to create an unusual ground state as observed in d-electron dimer systems where one of the triplet components parallel to the field is considered to play an important role as a hard-core boson.[7] In the d-electron dimer systems, two representative cases determined by the balance between the kinetic energy and the repulsive interactions have been intensively studied. When the kinetic energy is dominant, the triplet excited states are highly dispersive. The magnetization shows a kink at a critical magnetic field H_c and then shows a continuous rise, the region of which is regarded as a field-induced ordered phase (FIOP), up to the saturated magnetization, as observed in $TlCuCl_3$, $Ba_3Cr_2O_8$, and $BaCuSi_2O_6$.[8–11] When the repulsive interaction between neighboring bosons dominates, the bosons localize and form a superlattice to minimize the repulsive interaction, which is exposed as magnetization plateaus as observed in $SrCu_2(BO_3)_2$.[12] Here, we would like to emphasize that such a ground state can be easily achieved in the f-electron quantum spin system by using a conventional superconducting magnet without the use of the ultra-high-field magnet facility because of the weaker exchange interaction in the f-electron system compared to that in the d-electron system, although lower temperature is necessary.

It is noticeable that although the situation of $YbAl_3C_3$ seems to be similar to that of the d-electron dimer system, there may be an intrinsic difference between them. The Kramers doublet ground state in $YbAl_3C_3$ is an admixture of orbital and spin states, which leads to highly anisotropic g factor due to the CEF effect in the response for the magnetic field, while the quantum spin state in the d-electron system is close to a pure spin state in many cases. Therefore, the dimer state in $YbAl_3C_3$ may do a response different from the d-electron dimer system to the magnetic field. Consequently, it may be brought to an unprecedented quantum state different from the above-mentioned two cases. To explore a quantum state related to the $4f$-electron nature, we have investigated magnetic properties of $YbAl_3C_3$ under magnetic fields.

In this paper, first, we present history-dependent magnetic properties possibly ascribed to the cross correlation between the crystal deformation and the magnetic field, which were found in the process of exploring new quantum phases in $YbAl_3C_3$. Second, we present the emergence of unusual quantum states under magnetic fields, which may be in close relation with the characteristic nature of the $4f$-electron dimer system.

II. EXPERIMENTS

Single crystals of $YbAl_3C_3$ used in the present experiment were taken from the same batch as that reported in Ref. 3. Since the size of the single crystal of $YbAl_3C_3$ was very small (thin hexagonal plate of several hundreds of micrometers in diameter), several pieces of single crystals aligned in the same orientation were used for the magnetization (M) and specific-heat (C) measurements. The measurement of M in the range from 1.8 K to room temperature was carried out using a superconducting quantum interference device (SQUID) magnetometer. M at low temperatures down to $T \approx 0.5$ K was measured up to $H = 8$ T by the Faraday balance technique using a superconducting magnet with a field gradient. C down to $T \approx 0.5$ K was measured by the relaxation method using a commercial instrument (PPMS, Quantum Design Inc.). It should be noted that H means external magnetic field.

III. RESULT AND DISCUSSION

A. History-dependent magnetic properties in $YbAl_3C_3$

Figure 2 shows the temperature dependences of the magnetization of $YbAl_3C_3$ divided by magnetic field measured in magnetic fields along the a axis $[M_a(T)/H]$ and those measured in magnetic fields along the c axis $[M_c(T)/H]$ above $T = 1.8$ K. Here, the a and c axes refer to the hexagonal structure above $T_s = 77$ K. We found history-dependent magnetic properties in $YbAl_3C_3$. As understood from the main panel of Fig. 2, there arise distinct differences between zero-field cooled (zfc) $M_a(T)/H$ and field cooled (fc) $M_a(T)/H$ in both $H = 6$ and 7 T below $T_S = 77$ K, although no difference between zfc and fc $M_a(T)/H$ in $H = 1$ T was observed as reported previously.[3] Here, zfc $M_a(T)/H$ means those measured in heating just after zero-field cooling, whereas fc $M_a(T)/H$ means those measured in cooling under the magnetic field. These history-dependent phenomena are observed when a magnetic field $H \gtrapprox 3$ T is applied along the a axis. Similar behavior is also observed in $M_{a^*}(H)/H$ measured in a magnetic field along the a^* axis that is perpendicular to the a and c axes (not shown); however, $M_c(T)/H$ measured in a magnetic field along the c axis never shows such a behavior, even when a magnetic field of $H = 7$ T is applied, as shown in Fig. 2. Here, we pay attention to zfc $M_a(T)/H$ in $H = 1$, 6, and 7 T. In the frame of the dimer model, the field variation of zfc $M_a(T)/H$ below 10 K should be interpreted to be owing to the Zeeman splitting of the excited triplet state, and with increasing temperature greater than the energy scale of the Zeeman splitting, $M_a(T)/H$ should no longer depend on the strength of the magnetic field. Actually, zfc $M_a(T)/H$ in $H = 1$, 6, and 7 T coincide with each other

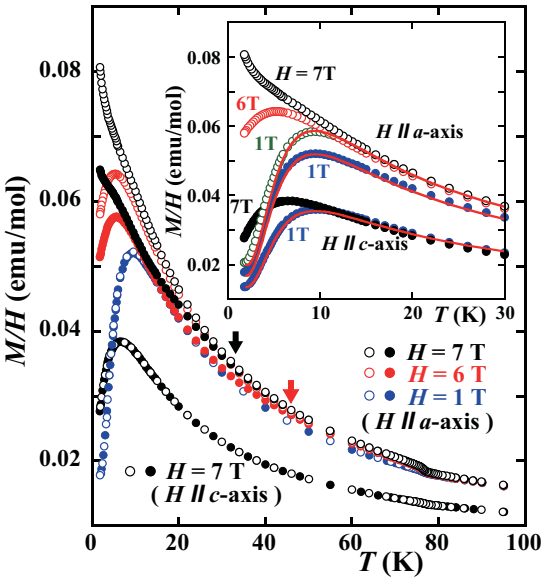

FIG. 2. (Color) Temperature dependence of zfc $M(T)/H$ (closed circles) and fc $M(T)/H$ (open circles) of $YbAl_3C_3$ measured in $H =$ 1, 6, and 7 T along the a axis and in $H = 7$ T along the c axis. Arrows indicate points where zfc $M_a(T)/H$ roughly coincides with fc $M_a(T)/H$ for $H = 6$ and 7 T. Inset shows a low-temperature part of $M_a(T)/H$. Blue closed circles show zfc $M_a(T)/H$ measured in $H = 1$ T, while green open circles show $M_a(T)/H$ measured in $H =$ 1 T in heating after cooling in $H = 7$ T from $T = 100$ K. Field cooled $M_a(T)/H$ measured in $H = 6$ and 7 T are labeled by red and black open circles, respectively. Zero-field cooled $M_c(T)/H$ measured in $H = 1$ (blue closed circles) and 7 T (black closed circles) along the c axis are also shown, which is not history dependent. Red solid curves display $M(T)/H$ calculated by an isolated dimer model of $S = 1/2$ spin pair using the parameters shown in Table I.

at $T \approx 15$ K; however, with further increasing temperature, zfc $M_a(T)/H$ in $H = 7$ T first and then that in $H = 6$ T deviate from the zfc $M_a(T)/H$ curve in $H = 1$ T, and then both approach the fc $M_a(T)/H$ curves measured in $H = 7$ and 6 T. Arrows in Fig. 2 indicate points where zfc $M_a(T)/H$ roughly coincides with fc $M_a(T)/H$ for each magnetic field along the a axis. Extrapolating the above-mentioned points to $T = 0$ K on the H-T plane, zfc and fc $M_a(T)/H$ are expected to coincide with each other even at $T = 0$ K by applying a magnetic field of $H \approx 10$ T at most.

Judging from the above-mentioned experimental results, two different kinds of magnetic states seem to emerge below T_s according to the strength of the magnetic field applied along the a axis. Therefore, we have examined the magnetic states brought by cooling in magnetic fields $H \gtrapprox 3$ T and $H < 3$ T. $M_a(T)/H$ measured in $H = 1$ T after cooling in a magnetic field of $H = 7$ T is shown by a green open circle in the inset of Fig. 2 accompanied with fc $M_a(T)/H$ measured in $H = 6$ and 7 T and zfc $M_a(T)/H$ measured in $H = 1$ T. $M_a(T)/H$ measured in $H = 1$ T after cooling in a magnetic field of $H =$ 7 T is apparently larger than zfc $M_a(T)/H$ in $H = 1$ T, and furthermore it coincides with fc $M_a(T)/H$ measured in $H =$ 6 and 7 T above $T = 15$ K different from zfc $M_a(T)/H$ in $H = 1$ T, as shown in the inset. This result indicates that the magnetic state brought by cooling in a high magnetic field

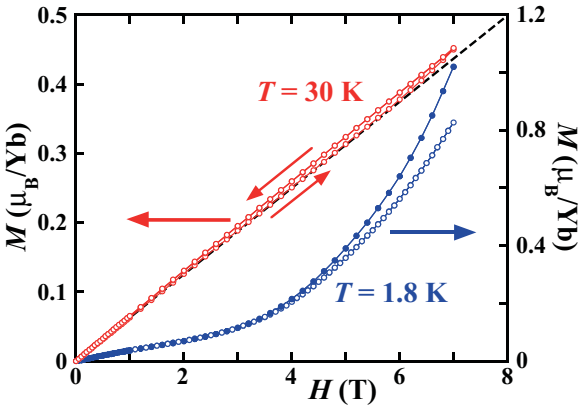

FIG. 3. (Color online) Field dependence of $M(H)$ measured in H along the a axis at $T = 1.8$ and 30 K. $M(H)$ measured after zero-field cooling are shown by open circles, and those measured after cooling in $H = 7$ T are indicated by closed circles. Initial $M(H)$ curve at $T = 30$ K just after zero-field cooling traces the lower curve; however, $M(H)$ after once exposed to $H = 7$ T traces the upper curve afterward.

along the a axis is different from that brought by cooling in a low magnetic field. On the other hand, when the magnetic field is applied along the c axis, both magnetic states brought by cooling in high and low magnetic fields seem to be the same. Actually, the temperature dependence of zfc $M_c(T)/H$ in $H = 7$ T is the same as that of fc $M_c(T)/H$ in $H = 7$ T as shown in the main panel of Fig. 2. Furthermore, zfc $M_c(T)/H$ in $H = 7$ T shows almost the same temperature dependence as that in $H = 1$ T above $T \approx 10$ K as shown in the inset of Fig. 2.

The history-dependent magnetic properties were also observed in the isothermal magnetization. Figure 3 shows the field dependences of the magnetization measured in magnetic fields along the a axis [$M_a(H)$] at $T = 1.8$ and 30 K. The $M_a(H)$ curve measured at $T = 1.8$ K after zero-field cooling (open circles) is distinctly different from that measured after cooling in $H = 7$ T (closed circles), and each traces each $M_a(H)$ curve in both increasing and decreasing fields. On the other hand, $M_a(H)$ at $T = 30$ K just after zero-field cooling first traces the lower curve in Fig. 3 with increasing field; however, after once exposed to $H = 7$ T at $T = 30$ K, $M_a(H)$ always traces the upper curve in both increasing and decreasing fields. Here, we would like to pay attention to the initial $M_a(H)$ curve after zero-field cooling traces the dotted straight line shown in Fig. 3 up to 6 T and then gradually deviates from it. This seems to correspond to the field variation of zfc $M(T)/H$ at $T = 30$ K displayed in Fig. 2, i.e., the value of zfc $M(T = 30/\mathrm{K})/H$ in $H = 6$ T is almost the same as that in $H = 1$ T but different from that in $H = 7$ T.

To interpret these experimental results, it is notable that the history-dependent phenomena are observed not in the high-temperature hexagonal phase, but in the low-temperature orthorhombic phase. Therefore, it is reasonable to assume that the history-dependent phenomena are in a close relation to the structural transition. Next, we note that the magnetic state brought by the cooling across T_s in a high magnetic field differs from that brought by the zero-field cooling. These features are partially similar to those observed in another

$4f$-electron quantum spin system Yb_4As_3 where the cooling across the structural transition temperature in uniaxial pressure stabilizes one among four kinds of structural domains.[13] In this case, since the crystal deformation from the cubic to trigonal one occurs by the shrinkage along the [111] or its equivalent directions, the structural domain with the principal axis in the same direction as that of the uniaxial pressure is chosen by applying the uniaxial pressure. On the assumption that the magnetic field in $YbAl_3C_3$ performs a role of the uniaxial pressure in Yb_4As_3, we may deduce that the states brought by the field and zero-field cooling in $YbAl_3C_3$ correspond to monodomain and multidomain states, respectively. Actually, three kinds of orthorhombic domains of $YbAl_3C_3$ are confirmed to arise in the low-temperature phase by the x-ray diffraction measurement in $H = 0$ T.[4] If our conjecture is correct, the field dependence of $M_a(H)$ at $T = 30$ K is understood to be ascribed to the fact that the sample exposed to $H = 7$ T falls into the monodomain state and it can not be returned to the multidomain state by the magnetic field alone. The absent history dependence in $M_c(T)$ can be also convinced because the fundamental translation vector along the c axis in the three orthorhombic domains is the same as that in the hexagonal phase. In order to confirm our deduction, x-ray diffraction measurement under the magnetic field using a single crystal is necessary, the study of which is now in progress.

Here, we would like to emphasize that the structural domains can be aligned by a magnetic field of 10 T at most even at very low temperatures if our conjecture is correct. In contrast to the case of Yb_4As_3 where the normal correlation between the structural deformation, i.e., the strain, and the uniaxial pressure, i.e., the stress, is observed, the structural deformation responsible for the magnetic field in $YbAl_3C_3$ suggests the cross correlation similar to those observed in multiferroic materials,[14–16] although $YbAl_3C_3$ below T_s is not in the ferromagnetic state but certainly in the dimer state. Since the application of a huge magnetic field of 30 T is reported to shift T_s of $YbAl_3C_3$ by about 10 K, some linkage between the crystal deformation and the magnetic field is reasonably expected.[17] One of the possible explanations for such a cross correlation may be owing to the different Zeeman energy gains among the field directions due to the anisotropic magnetic susceptibility; however, it is hardly considered that such a narrow margin of the magnetic susceptibilities dominates the lattice deformation. Therefore, another way to combine the strain and the magnetic field may be necessary such as a large magnetostrictive effect as proposed in $Tb_2(MoO_3)_4$, although the present case seems to be much stronger.[18]

Next, we examine whether the magnetic susceptibility of the monodomain state can be reproduced by the simple isolated dimer model in the same way as Ref. 3. Red lines in the inset of Fig. 2 display the fitting curves for $M(T)/H$ measured in $H = 1$ T assuming the isolated dimer model composed of $S = 1/2$ spin pair with anisotropic g factor where fitting parameters are Van Vleck–type paramagnetic susceptibility (χ_v) and a contribution from magnetic impurities (C_i/T) in addition to a singlet-triplet splitting energy (Δ) and g factor. χ_v is supposed to be a contribution from the CEF excited state being mixed in by the application of the magnetic field. As understood from the inset of Fig. 2, the magnetic susceptibility of the monodomain state is well reproduced by the isolated dimer model as well as that in the multidomain state. Values of the parameters obtained by this fitting are displayed in Table I. The parameters for $M_c(T)/H$ and $M_a(T)/H$ in the multidomain state are almost the same as those in Ref. 3 except for C_i. The variation of C_i in Table I is probably ascribed to the oxidation because the sample was repeatedly used. The g factor for $M_a(T)/H$ in the monodomain state is larger than that in the multidomain state, reflecting the anisotropic magnetic susceptibility on the c plane due to the CEF effect.

TABLE I. Parameters used for the fitting of $M(T)/H$ measured in $H = 1$ T in the inset of Fig. 2 assuming an isolated dimer model composed of the $S = 1/2$ spin pair.

	Δ (K)	g factor	χ_v (emu/mol)	C_i (emu K/mol)
$H \| c$	15.5	2.26	0.010	0.006
$H \| a$(multidomain)	15.5	2.86	0.011	0.010
$H \| a$(monodomain)	15.5	3.07	0.011	0.016

B. Low-temperature magnetic properties of $YbAl_3C_3$

1. Fields parallel to the a axis

When the magnetic field is applied on $YbAl_3C_3$ along the a axis at low temperatures, something is expected to happen around $H = 7.5$ T in the monodomain state where the energy of one of the excited states is predicted to cross that of the ground state by the isolated dimer model mentioned before. Figure 4(a) shows the field dependence of the magnetization at low temperatures after subtracting a contribution of the Van Vleck–type paramagnetism in a field along the a axis $[M_a(H)\text{-}\chi_{va}H]$ where the value of χ_{va} listed in Table I was used. $M_a(H)$ was measured after cooling in $H = 7$ T to align the structural domains in the same direction. Although $M_a(H)\text{-}\chi_{va}H$ at $T = 1.8$ K seems to vary smoothly as a function of the magnetic field, the structure in $M_a(H)\text{-}\chi_{va}H$ is gradually visible with decreasing temperature. $M_a(H)\text{-}\chi_{va}H$ at $T = 0.47$ K is almost zero at low fields and then shows a clear kink around $H = 4.5$ T. This value of the magnetic field, 4.5 T, is much lower than the value of 7.5 T predicted by the isolated dimer model. Above $H = 4.5$ T, $M_a(H)\text{-}\chi_{va}H$ shows a continuous rise linear with H, and then exhibits a sudden increase around $H = 6.6$ T, suggesting a metamagnetic transition although any hysteresis around $H = 6.6$ T is not observed down to $T = 0.47$ K. The structure of $M_a(H)\text{-}\chi_{va}H$ implies the existence of three magnetic phases. The magnetic phase below $H \approx 4.5$ T is certainly characterized by the dimer state, while that above $H \approx 6.6$ T may be a polarized phase where the magnetic moment is almost fully polarized because $M_a(H)\text{-}\chi_{va}H = 1.3\mu_B$ at $H = 8$ T is close to $g\mu_B/2 = 1.53\mu_B$ of the saturated magnetic moment in the monodomain state predicted by the dimer model. At this stage, it is reasonable to think that the intermediate phase between the above-mentioned two phases corresponds to a field-induced ordered phase observed in the d-electron dimer system such as $TlCuCl_3$, $Ba_3Cr_2O_8$, and $BaCuSi_2O_6$.[8–11] The kink of $M_a(H)\text{-}\chi_{va}H$ around $H = 4.5$ T is thought to be an emergence of the magnetization when entering FIOP. Hence, the position of

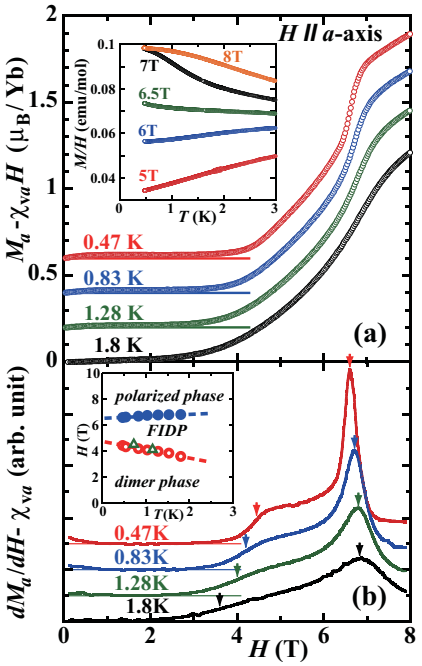

FIG. 4. (Color online) (a) Field dependence of the magnetization of $YbAl_3C_3$ measured in $H \| a$ after subtracting the contribution of the Van Vleck–type paramagnetism [$M_a(H)$-$\chi_{va}H$]. Each magnetization curve is shifted along the vertical axis by multiplicative factors of $0.2\mu_B$. Inset shows the temperature dependence of $M_a(T)/H$ measured in $H \| a$ down to $T \approx 0.5$ K. (b) Field derivative of the magnetization of $YbAl_3C_3$ measured in $H \| a$ after subtracting the contribution of the Van Vleck–type paramagnetism (dM_a/dH-χ_{va}). Arrows in the high-field region from 6 to 7 T indicate peaks of dM_a/dH-χ_{va}, and those in the low-field region from 3 to 5 T show peak positions of d^2M_a/dH^2. Inset shows magnetic phase diagram of $YbAl_3C_3$ under the magnetic field along the a axis. Circles and triangles are obtained from the magnetization and specific-heat measurements, respectively.

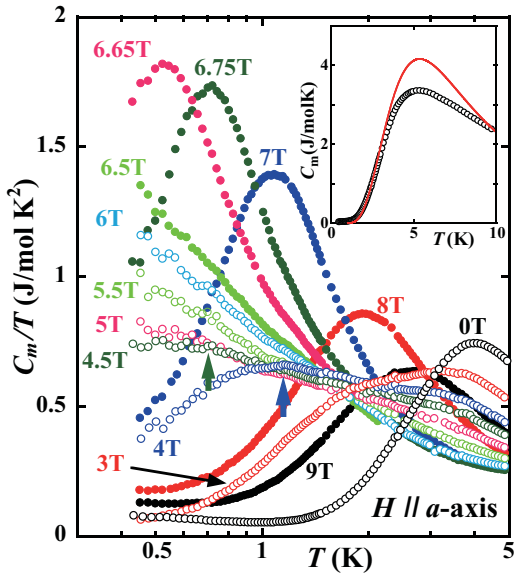

FIG. 5. (Color online) Temperature dependence of the magnetic specific heat of $YbAl_3C_3$ divided by the temperature (C_m/T) measured in a magnetic field along the a axis. Inset compares experimental values of C_m (open circles) at $H = 0$ T and calculated C_m values by the simple dimer model (solid line).

the kink seems to suggest the dispersive triplet state, which is probably ascribed to a significant interdimer interaction.[19] On the other hand, the sudden increase of $M_a(H)$-$\chi_{va}H$ at $H =$ 6.6 T seems not to be usual.

To clarify whether FIOP really exists or not in $YbAl_3C_3$, the temperature dependence of $M(T)$ was measured. In the inset of Fig. 4(a), the temperature dependences of $M_a(T)/H$ in various magnetic fields down to $T \approx 0.5$ K are displayed. Unexpectedly, no distinct anomaly indicating FIOP in $M_a(T)/H$ could be found, which offers a remarkable contrast with the observation of the clear cusp in $M(T)$ in the d-electron dimer systems such as $TlCuCl_3$.[20]

We differentiated $M_a(H)$ by H to reveal the boundary between each magnetic phase. Figure 4(b) shows the field derivative of the magnetization of $YbAl_3C_3$ measured in $H \| a$ after subtracting the contribution of the Van Vleck–type paramagnetism (dM_a/dH-χ_{va}). Steplike changes in the vicinity of $H = 4$ T are observed in the field dependence of dM_a/dH-χ_{va} corresponding to the emergence of the magnetic moments; however, they seem to be too gradual to regard them as second-order phase transitions. We consider peak positions of second derivative of M_a by H as a border between the dimer phase and the intermediate phase, which are indicated by arrows around $H = 4$ T in the lower panel of Fig. 4. Meanwhile, dM_a/dH-χ_{va} make sharp peaks corresponding to the abrupt increase of M_a, which are indicated by arrows and suggest a first-order phase transition although no hysteresis was observed as mentioned before.

By summarizing the above-mentioned points, the H-T phase diagram was obtained as shown in the inset of Fig. 4(b). Here, we would like to emphasize that the intermediate phase is not closed and tends to expand with increasing temperature, being in a marked contrast to FIOP observed in the d-electron dimer system.[11,21,22]

To get a deeper insight into the nature of each magnetic phase in $YbAl_3C_3$, the specific-heat measurement was performed at low temperatures. Figure 5 shows the temperature dependence of the magnetic specific heat of $YbAl_3C_3$ divided by the temperature (C_m/T) measured in $H \| a$. The magnetic specific heat of $YbAl_3C_3$ was obtained by subtracting the specific heat of $LuAl_3C_3$ from that of $YbAl_3C_3$. One may be aware of three typical behaviors in the temperature dependence of C_m/T corresponding to the above-mentioned three magnetic phases. At $H = 0$ T, a broad peak of C_m/T around $T = 4$ K appears, which can be explained by the thermal excitation from the singlet ground state to the triplet excited state, i.e., a Schottky-type peak. In the inset of Fig. 5, C_m of $YbAl_3C_3$ at $H = 0$ T (open circles) and C_m calculated using the dimer model (solid line) are shown. The calculated C_m curve is sharper and higher than the experimental C_m curve. This discrepancy could be interpreted to be due to the dispersive energy level of the triplet excited sate, which implies a considerable interdimer interaction as mentioned before. By applying the field of $H = 3$ T, C_m/T becomes broader because one of the triplet components approaches the singlet ground state. On the other hand, C_m/T in the high-field

region of $H = 7$, 8, and 9 T forms a Schottky-type peak again. The fact that the peak temperature increases with increasing field is reasonably explained by the level crossing between the initial ground state and one of the triplet components, i.e., the Schottky-type peak is ascribed to the thermal excitation from one of the triplet components to the initial singlet ground state. The reason why the level crossing occurs at lower field than $H = 7.5$ T predicted by the isolated dimer model is considered to be relevant to the sudden change in $M(H)$ around $H = 6.6$ T, although the origin of the sudden change in $M(H)$ is not clear at this stage.

In contrast to the above-mentioned two phases, the intermediate phase shows rather characteristic temperature dependence of C_m/T. As understood from Fig. 5, no evident peak suggesting the phase transition to FIOP is observed. Instead, anomalous increases of C_m/T in proportion to $-\ln T$ are observed in the field range from $H = 5$ to 6.5 T. Such anomalous increases of C_m/T suggest that a highly disordered state consisting of the initial singlet ground state and one of the triplet components distributed over a finite field range from $H = 5$ to 6.5 T endures down to low temperatures. Hereafter, we call this region a field-induced disordered phase (FIDP).

Next, we reexamine the boundaries between the above-mentioned three magnetic phases. Judging from the H-T phase diagram shown in the inset of Fig. 4(b), the C_m/T curve measured in $H = 4$ T and also probably that in $H = 4.5$ T are expected to cross the boundary between the dimer phase and FIDP. Although no evident peak suggesting a phase transition is observed, with decreasing temperature the C_m/T curves measured in $H = 4$ and 4.5 T change their temperature dependence from $-\ln T$ at $T \approx 1.1$ and 0.7 K, respectively. Such points are shown by arrows in Fig. 5 and are plotted by open triangles in the H-T phase diagram shown in the inset of Fig. 4(b). They are in good agreement with the boundary determined by the magnetization measurement. Considering the gradual steplike change in dM_a/dH-χ_{va} and the missing of the sharp peak in C_m/T, the boundary between the dimer phase and FIDP is considered to be a crossover line.

In comparison to the boundary between FIDP and the dimer phase, detection of the boundary between FIDP and the polarized phase by the $C(T)$ measurement seems to be difficult because its boundary in the H-T phase diagram is almost parallel to the transverse temperature axis as shown in the inset of Fig. 4(b). Actually, any evidence that C_m/T crosses the boundary seems not to be observed. Nevertheless, it is possible to determine the boundary because each characteristic of each phase observed in C_m/T is distinctly different, i.e., $-\ln T$ behavior in FIDP and the Schottky-type peak in the polarized phase. Hence, the boundary line is deduced from Fig. 5 to be located in a very tiny field range around $H = 6.6$ T, where the $M_a(H)$ curve shows a discontinuous change. Considering that the discontinuity of the $M_a(H)$ curve is somewhat blunt and has no hysteresis, it is reasonably assumed that the boundary between FIDP and the polarized phase seems to be a crossover relevant to a first-order phase transition.

Recently, FIOP in the d-electron dimer system has attracted much attention of many researchers because it is regarded as Bose-Einstein condensation (BEC) when the field is applied along the symmetry axis of U(1).[23] If the U(1) symmetry is broken by antisymmetric spin interactions or a staggered component of the g tensor, the phase transition is no longer expected. The influence of the same type of anisotropy has been investigated in a Haldane spin chain of $Ni(C_2H_8N_2)_2NO_2(ClO_4)$, abbreviated NENP, where no phase transition is observed in spite of the emergence of magnetic moments at a critical field similar to that of FIOP.[24,25] Instead, nonzero spin gap is observed to remain even above the critical field, which signifies the existence of the anticrossing due to the mixing between the ground state and the excited state caused by the staggered component of the g tensor. Therefore, we pay attention to which Yb-ion pair forms the dimer state in the orthorhombic phase of $YbAl_3C_3$. Below T_s, Yb-Yb bonds are reported to be classified into four types as shown in Fig. 1(b).[4] Two types [J_3 and J_4 in Fig. 1(b)] among these are excluded from candidates for the dimer because they connect with the same type of the bond and consequently form a chain of magnetic Yb ions. The other two types [J_1 and J_2 in Fig. 1(b)] have the inversion center in the middle of each Yb-Yb bond. Therefore, both anisotropic effects do not work in $YbAl_3C_3$. Actually, any sign of spin gap is not detected in FIDP of $YbAl_3C_3$. On the other hand, the U(1) symmetry is also broken by a single-ion anisotropy, which can be applicable for $YbAl_3C_3$ in a field along the a axis because the CEF anisotropy around the a axis is very large. However, the physical properties predicted by the theory and those actually observed in the d-electron dimer seem to provide a striking contrast to those of $YbAl_3C_3$.[23,26] At the present stage, although the origin of $-\ln T$ dependence of C_m/T extended over a finite magnetic field range is still puzzling, it may be relevant to the characteristic magnetic state of the $4f$-electron as mentioned before.

It is noticeable that the same temperature dependence of C_m/T is often observed in the so-called strongly correlated $4f$-electron system such as Ce-based compounds. In these compounds, a second-order phase transition at $T = 0$ K occurs from the magnetically ordered state to the nonmagnetic heavy-fermion state through a quantum critical point (QCP) by tuning control parameters of pressure, magnetic field, and so on.[27] The logarithmic increase of C_m/T is observed in the vicinity of the singular point of QCP and is regarded as non-Fermi-liquid behavior.[28,29] In the heavy-fermion state, the spin of the conduction electron couples with the spin of the $4f$-electron forming the nonmagnetic singlet state by the Kondo effect. This situation may correspond to the dimer state of $YbAl_3C_3$ where the intradimer interaction plays a role of the Kondo effect. However, in contrast to that non-Fermi-liquid behavior converges to QCP with decreasing temperature, it is unconventional that FIDP in $YbAl_3C_3$ is distributed over a finite field range even at low temperatures.

2. *Fields parallel to the c axis*

When the magnetic field is applied along the c axis, an unconventional magnetic phase similar to FIDP in $H \| a$ is also expected to be induced. Figure 6(a) shows the field dependence of the magnetization below $T = 1.8$ K after subtracting a contribution of the Van Vleck–type paramagnetism in a field along the c axis [$M_c(H)$-$\chi_{vc}H$] where the value of χ_{vc} in Table I was used. The convex shape of $M_c(H)$-$\chi_{vc}H$ around $H = 0$–1 T, which becomes apparent with decreasing

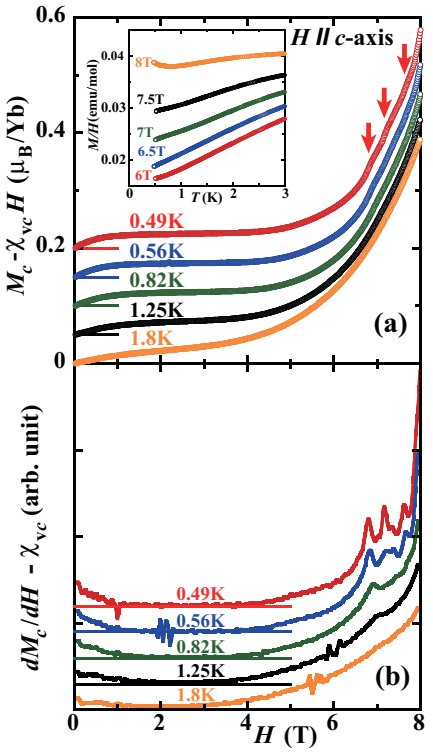

FIG. 6. (Color online) (a) Field dependence of the magnetization of $YbAl_3C_3$ measured in $H\|c$ after subtracting the contribution of the Van Vleck–type paramagnetism [$M_c(H)$-$\chi_{vc}H$]. Each magnetization curve is shifted along the vertical axis by multiplicative factors of $0.05\mu_B$. Arrows indicate peak positions of dM_c/dH-χ_{vc} shown in the lower panel (b). Inset shows the temperature dependence of $M_c(T)/H$ measured in $H\|c$ down to $T \approx 0.5$ K. (b) Field derivative of the magnetization of $YbAl_3C_3$ measured in $H\|c$ after subtracting the contribution of the Van Vleck–type paramagnetism (dM_c/dH-χ_{vc}).

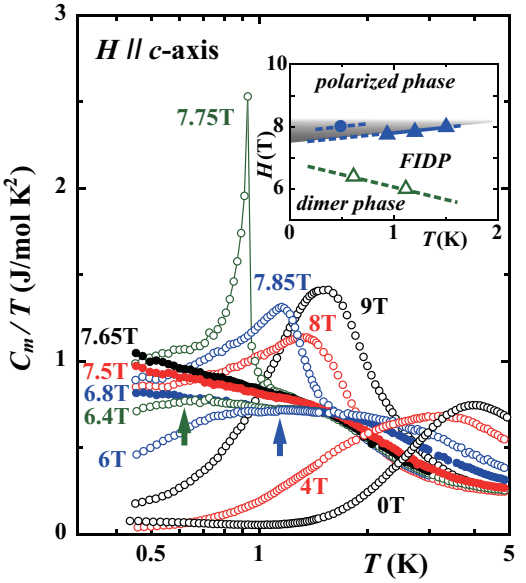

FIG. 7. (Color online) Temperature dependence of the magnetic specific heat of $YbAl_3C_3$ divided by the temperature (C_m/T) measured in $H\|c$. Inset shows H-T phase diagram of $YbAl_3C_3$ in $H\|c$. A closed circle corresponds to the abrupt increase of M_c around $H = 8$ T, while closed and open triangles are determined by the specific-heat measurement. Shaded region is a new field-induced disordered phase (NFIDP) characterized by the large C_m/T value, although its boundary is not accurate at the present stage.

temperature, is probably attributed to the isolated Yb^{3+} ions yielded by the oxidation because the sample was repeatedly used as mentioned before. $M_c(H)$-$\chi_{vc}H$ shows a kink around $H = 5$–6 T, which is similar to that of $M_a(H)$-$\chi_{va}H$ at $H = 4.5$ T but somewhat gradual. An abrupt increase in $M_c(H)$-χ_{vc} similar to that in $M_a(H)$-$\chi_{va}H$ at $H = 6.6$ T is observed around $H = 8$ T at $T = 0.49$ K. Therefore, magnetic phases of $YbAl_3C_3$ in a field along the c axis are considered to be also divided into three regions of the dimer phase, the intermediate phase, and probably the polarized phase above $H = 8$ T, on the analogy of the case measured in a field along the a axis, although the border line between the dimer phase and the intermediate phase is not clear compared to that in a field along the a axis.

To check whether the intermediate phase is FIOP or not, the temperature dependence of $M(T)$ in fields along the c axis was measured in the same way as those measured in fields along the a axis. Inset of Fig. 6(a) displays the temperature dependence of $M_c(T)/H$ down to $T \approx 0.5$ K where no distinct anomaly indicating FIOP in $M_c(T)/H$ could be found except an upturn at low temperature in $H = 8$ T as well as the case measured in a field along the a axis.

In contrast to the smoothly varying M_a-$\chi_{va}H$ in the FIDP region, M_c-$\chi_{vc}H$ above $H \approx 6$ T at $T = 0.49$ K seems to have a fine structure when examining it in detail, although it is not clear. Hence, we differentiated $M_c(H)$ by H to clarify the fine structure. Figure 6(b) shows the field derivative of the magnetization of $YbAl_3C_3$ measured in $H\|c$ after subtracting the contribution of the Van Vleck–type paramagnetism (dM_c/dH-χ_{vc}). Three peaks at least in dM_c/dH-χ_{vc} seem to be visible and shift to low-field side with decreasing temperature. On the other hand, there is seen the left half of the peak around $H = 8$ T in dM_c/dH-χ_{vc} at $T = 0.49$ K, which seems to shift to high-field side and to become broader with increasing temperature. It should be noted that the the peak around $H = 8$ T is much larger than three peaks, suggesting a different character between the peak around $H = 8$ T and the three peaks. The peak around $H = 8$ T reflects the abrupt increase in $M_c(H)$-$\chi_{vc}H$, which resembles the abrupt increase in $M_a(H)$-$\chi_{va}H$ at $H = 6.6$ T, while the three peaks recall us to the magnetization plateaus such as those observed in $SrCu_2(BO_3)_2$.[12] Actually, three small steps of $M_c(H)$-$\chi_{vc}H$, which are indicated by arrows, can be barely seen at $T = 0.49$ K. Assuming the saturated magnetic moment of $g\mu_B/2 = 1.13\mu_B$ along the c axis predicted by the dimer model, fractional rates of the first, second, and third plateaus are roughly estimated to be 1/8, 1/6, and 1/4, respectively.

Figure 7 shows the temperature dependence of the magnetic specific heat of $YbAl_3C_3$ divided by the temperature (C_m/T) measured in $H\|c$. Three typical behaviors in the temperature dependence of C_m/T corresponding to the above-mentioned three magnetic phases are remarked as well as the case measured in $H\|a$, i.e. Schottky-type peak at $H = 0$ and 4 T ascribed to the thermal excitation from the singlet ground state

to the triplet excited state in the dimer phase, $-\ln T$ behavior in the field range from $H = 6.8$ to 7.65 T in FIDP of the intermediate phase, and Schottky-type peak around $H = 9$ T due to the thermal excitation from one of the triplet components to the initial singlet ground state in the polarized phase. The boundary between the dimer phase and FIDP, which could not be strictly drawn by the magnetization measurement as stated before, was determined by the C_m/T curves as well as the case measured in $H \| a$. When crossing the boundary, the C_m/T curves measured in $H = 6$ and 6.4 T change their temperature dependence from $-\ln T$ at $T \approx 1.1$ and 0.6 K shown by arrows in Fig. 7, respectively. The absence of the sharp peak in C_m/T at the boundary between the dimer phase and FIDP implies that the boundary is a crossover line as well as the case measured in $H \| a$. On the other hand, a sharp peak of C_m/T at $H = 7.75$ T is in contrast to those observed in $H \| a$. This peak clearly indicates a phase transition at $T = 0.93$ K under $H = 7.75$ T. When the magnetic field increases from 7.75 to 8 T, this peak seems to shift to higher-temperature side and becomes broader. But, it should be noted that these C_m/T peaks seem to be qualitatively different in the shape from that at $H = 9$ T. C_m/T at $H = 7.75$, 7.85, and 8 T maintain a huge value of about 1 J/molK^2, which implies a certain kind of remaining disorder, even at considerably lower temperature than the peak temperature, while C_m/T at $H = 9$ T below the peak temperature steeply decreases with decreasing temperature. Assuming that the C_m/T peak at $H = 9$ T is a Schottky peak in the polarized phase, a new field-induced disordered phase (NFIDP) characterized by a huge C_m/T value is deduced to appear between FIDP and the polarized phase. Considering the shape of the C_m/T peak, this transition from FIDP to NFIDP seems to be a first-order transition at low temperatures and then changes to a crossover with increasing temperature. The boundary between NFIDP and the polarized phase is possibly located from $H =$ 8 to 9 T.

In the meantime, we could not find any anomaly of the specific heat relevant to the magnetization plateaus. Several possibilities are mentioned as its reason. One possibility is that the field direction is somewhat deviated from the c axis as described later. If the field direction is inclined from the c axis by 90°, i.e., being parallel to the a axis, no sign of the magnetization plateaus is expected as seen in Fig. 4. The other possibility is that the boundary of the magnetic phase relevant to the magnetization plateaus is located on the much lower-temperature side than the minimum temperature of the measurement or it is a crossover line. To clarify these issues, much precise measurement in the lower-temperature region is desired, which is now in progress.

Based on the above discussion, the H-T phase diagram in the field along the c axis shown in the inset of Fig. 7 is drawn. Shaded region in the H-T phase diagram is NFIDP characterized by the large C_m/T value below its peak temperature, although it is somewhat not clear where the boundary between NFIDP and the polarized phase is. The peak positions of C_m/T at $H = 7.75$, 7.85, and 8 T are shown by closed triangles, and a closed circle corresponds to the abrupt increase of M_c around $H = 8$ T. Although we suppose that these points should be on the same line, i.e., the boundary between FIDP and NFIDP, the closed circle slightly deviates from the extrapolation of the closed triangles. This discrepancy between the magnetization and specific-heat measurements is probably ascribed to the anisotropic magnetization between the c and a axes. In the specific-heat measurement, the c axis might be inclined somewhat from the field direction probably due to the anisotropic magnetization in this magnetic field region. Therefore, the actual boundary line between FIDP and NFIDP is considered to locate at somewhat higher-field side than that determined by the specific-heat measurement, i.e., on the closed circle determined by the magnetization measurement. On the other hand, the boundary between the dimer phase and FIDP determined by the specific heat, which are shown by open triangles in the inset of Fig. 7, may reflect the accurate position because both magnetizations along the a and c axes are not so large in this field region. As understood from the H-T phase diagram, FIDP in $H \| c$ is not closed as well as the case measured in $H \| a$. Comparing the H-T phase diagrams in the field along the a and c axes, one may be aware that the FIDP region in $H \| c$ is narrower than that in $H \| a$ at $T = 0$ K even considering the ambiguity of the boundary. Meanwhile, NFIDP is characteristic in a field along the c axis because it is not observed in a field along the a axis. Furthermore, the large C_m/T value in the new disordered phase indicates that the disorder remains even at low temperatures. Combining FIDP and NFIDP, an anomalous disordered region is considered to spread over a finite field range at $T = 0$ K even in a field along the c axis, which may be also characteristic of the 4f-electron nature as well as the case in a field along the a axis.

IV. CONCLUSION

Magnetic properties of a spin-gap material $YbAl_3C_3$ have been investigated. We have found the history-dependent magnetization, which suggests the cross correlation between the structural deformation and the magnetic field similar to those observed in multiferroic materials although $YbAl_3C_3$ below T_s is not in the ferromagnetic state. The structural monodomain state is expected to be realized by applying a magnetic field of $H \geqslant 10$ T even at low temperatures. On the other hand, the field dependence of $M(H)$ in $YbAl_3C_3$ at low temperatures shows similar behaviors to those of FIOP in the d-electron dimer systems. However, neither kink nor peak suggesting the emergence of FIOP is observed in the temperature dependence of both $M(T)$ and $C(T)$ except a field range of $H = 7.75$–8 T along the c axis. Instead, C_m/T shows an anomalous increase proportional to $-\ln T$ with decreasing temperature in a finite field range, suggesting an anomalous disordered state such as a non-Fermi-liquid state in a strongly correlated f-electron system. These anomalous characteristics different from those of the d-electron dimer system may be relevant to the nature of the f electron.

ACKNOWLEDGMENTS

The authors would like to thank H. Moriyama, M. Kikuchi, and M. Suzuki for their technical support. This work was supported by a Grant-in-Aid for Scientific Research (B) (Grant No. 20340083).

*aochiai@mail.clts.tohoku.ac.jp

[1]M. Kohgi, K. Iwasa, J.-M. Mignot, A. Ochiai, and T. Suzuki, Phys. Rev. B **56**, R11388 (1997).
[2]T.-M. Gesing, R. Pöttgen, W. Jeitschko, and U. Wortmann, J. Alloys Comp. **186**, 321 (1992).
[3]A. Ochiai, T. Inukai, T. Matsumura, A. Oyamada, and K. Katoh, J. Phys. Soc. Jpn. **76**, 123703 (2007).
[4]T. Matsumura, T. Inami, M. Kosaka, Y. Kato, T. Inukai, A. Ochiai, H. Nakao, Y. Murakami, S. Katano, and H. S. Suzuki, J. Phys. Soc. Jpn. **77**, 103601 (2008).
[5]S. K. Dhar, P. Manfrinetti, M. L. Fornasini, and P. Bonville, Eur. Phys. J. B **63**, 187 (2008).
[6]Y. Kato, M. Kosaka, H. Nowatari, Y. Saiga, A. Yamada, T. Kobiyama, S. Katano, K. Ohyama, H. S. Suzuki, N. Aso, and K. Iwasa, J. Phys. Soc. Jpn. **77**, 053701 (2008).
[7]T. M. Rice, Science **298**, 760 (2002).
[8]T. Nikuni, M. Oshikawa, A. Oosawa, and H. Tanaka, Phys. Rev. Lett. **84**, 5868 (2000).
[9]F. Yamada, T. Ono, H. Tanaka, G. Misuguich, M. Oshikawa, and T. Sakakibara, J. Phys. Soc. Jpn. **77**, 013701 (1999).
[10]M. Kofu, H. Ueda, H. Nojiri, Y. Oshima, T. Zenmoto, K. C. Rule, S. Gerischer, B. Lake, C. D. Batista, Y. Ueda, and S.-H. Lee1, Phys. Rev. Lett. **102**, 177204 (2009).
[11]M. Jaime, V. F. Correa, N. Harrison, C. D. Batista, N. Kawashima, Y. Kazuma, G. A. Jorge, R. Stein, I. Heinmaa, S. A. Zvyagin, Y. Sasago, and K. Uchinokura, Phys. Rev. Lett. **93**, 087203 (2004).
[12]H. Kageyama, A. Onizuka, T. Yamauchi, Y. Ueda, S. Hane, H. Mitamura, T. Goto, K. Yoshimura, and K. Kosuge, J. Phys. Soc. Jpn. **68**, 1821 (1999).
[13]A. Ochiai, T. Suzuki, and T. Kasuya, J. Phys. Soc. Jpn. **59**, 4129 (1990).
[14]K. Aizu, J. Phys. Soc. Jpn. **27**, 387 (1969).
[15]M. Fukunaga, Y. Sakamoto, H. Kimura, Y. Noda, N. Abe, K. Taniguchi, T. Arima, S. Wakimoto, M. Takeda, K. Kakurai, and K. Kohn, Phys. Rev. Lett. **103**, 077204 (2009).
[16]M. H. Lente, J. D. S. Guerra, G. K. S. de Souza, B. M. Fraygola, C. F. V. Raigoza, D. Garcia, and J. A. Eiras, Phys. Rev. B **78**, 054109 (2008).
[17]T. Mito, S. Tomisawa, S. Wada, H. Harima, K. Hashi, T. Shimizu, A. Goto. S. Ohki, Y. Kato, and M. Kosaka, J. Phys. Soc. Jpn. **78**, 014709 (2009).
[18]B. K. Ponomarev, V. D. Negrii, B. S. Redfkin, and Yu. F. Popov, J. Phys. D: Appl. Phys. **27**, 1995 (1994).
[19]D. T. Adroja, K. A. McEwen, M. Kosaka, A. D. Hillier, J.-G. Park, and K. Kondo, ISIS Experimental Report No. RB920466, 2010.
[20]A. Oosawa, T. Takamasu, K. Tatani, H. Abe, N. Tsujii, O. Suzuki, H. Tanaka, G. Kido, and K. Kindo, Phys. Rev. B **66**, 104405 (2002).
[21]A. A. Aczel, Y. Kohama, M. Jaime, K. Ninios, H. B. Chan, L. Balicas, H. A. Dabkowska, and G. M. Luke, Phys. Rev. B **79**, 100409(R) (2009).
[22]S. E. Sebastian, P. A. Sharma, M. Jaime, N. Harrison, V. Correa, L. Balicas, N. Kawashima, C. D. Batista, and I. R. Fisher, Phys. Rev. B **72**, 100404(R) (2005).
[23]J. Sirker, A. Weisse, and O. P. Sushikov, Europhys. Lett. **68**, 275 (2004).
[24]K. Katsumata, H. Hori, T. Takeuchi, M. Date, A. Yamagishi, and J. P. Renard, Phys. Rev. Lett. **63**, 86 (1989).
[25]T. Kobayashi, Y. Tabuchi, K. Amaya, Y. Ajiro, Y. Yosida, and M. Date, J. Phys. Soc. Jpn. **61**, 1772 (1992).
[26]E. C. Samulon, Y.-J. Jo, P. Sengupta, C. D. Batista, M. Jaime, L. Balicas, and I. R. Fisher, Phys. Rev. B **77**, 214441 (2008).
[27]S. Doniach, Phys. B (Amsterdam) **91**, 231 (1977).
[28]H. v. Löhneysen, T. Pietrus, G. Portisch, H. G. Schlager, A. Schröder, M. Sieck, and T. Trappmann, Phys. Rev. Lett. **72**, 3262 (1994).
[29]B. Bogenberger and H. v. Löhneysen, Phys. Rev. Lett. **74**, 1016 (1995).